Evaluation of micromechanical methods to determine stiffness and strength properties of foams

Narendran Subramanian and Bhavani V Sankar

Journal of Sandwich Structures and Materials 2012 14: 431 originally published online 25 May 2012
DOI: 10.1177/1099636212441475

JOURNAL OF SANDWICH STRUCTURES & MATERIALS

Article

Journal of Sandwich Structures and Materials
14(4) 431–447

DOI: 10.1177/1099636212441475
jsm.sagepub.com
SAGE

Evaluation of micromechanical methods to determine stiffness and strength properties of foams

Narendran Subramanian and Bhavani V Sankar

Abstract

The stiffness and strength properties of foams with tetrakaidecahedral unit cells are evaluated using both finite element-based micromechanics and analytical methods. The finite element analysis models the varying cross section of the struts exactly. The analytical methods assume the struts have constant cross section along the length. Equivalent constant cross section of the strut can be obtained by either matching the densities or by using harmonic averaging of the stiffness properties. A method in which the moment of inertia of the cross section is averaged is also considered. The comparison of properties obtained for the different equivalent constant cross-section foams shows the inability of the various averaging schemes to match the shear modulus and the strength properties, while the Young's modulus matches to some extent. The failure of the weakest cross section in the varying cross-section strut of the unit cell leads to a lower tensile strength in the actual foam compared to the uniform cross-section foams. The results suggest that although the use of simple analytical models for foam properties are attractive, they often lead to erroneous results, and hence exact modeling of the strut geometry is key to estimating the stiffness and strength properties of foams and other cellular solids.

Keywords

Foams, sandwich construction, tetrakaidecahedral cell, finite element analysis, micromechanics, homogenization

Department of Mechanical & Aerospace Engineering, University of Florida, Gainesville, FL, USA

Corresponding author:
Bhavani V Sankar, Department of Mechanical & Aerospace Engineering, University of Florida, Gainesville, FL 32611, USA
Email: sankar@ufl.edu

Introduction

Currently, foams (Figure 1) of all types—polymeric, metallic, and ceramic foams—are used in sandwich construction. For example, metallic foams are used in thermal protection systems.[2] Ceramic foam sandwich construction is envisioned for the thermal protection systems of future space vehicles.[3,4] Cooling systems for aircraft and rocket engines use sandwich construction with open cell metallic foams for passing the cooling fluid.[5] With the recent advances in manufacturing techniques of foams and cellular solids, it is possible to tailor the properties of the foam based on their microstructural details. Thus, it is not necessary to only resort to experimental techniques to characterize the foams. Numerical simulations can be used to identify microstructures for achieving desired properties. Some of the properties that can be obtained using numerical simulations are stiffness, strength, fracture toughness, and thermal conductivity. Although computational methods such as finite element (FE)-based micromechanics are accurate and model very realistic microstructures, they are time-consuming. On the other hand, simple analytical methods can be used in the preliminary stages of design and also in optimizing the foam properties. When one is interested in determining the variability in the foam properties, a large number of Monte Carlo simulations are necessary for propagating uncertainties in the foam microstructure. In such cases, simple analytical methods are cost-effective as they can be used for thousands or even millions of analyses.

In this paper, we evaluate the analytical and FE models for stiffness and strength properties of tetrakaidecahedral foams. Analytical models are based on simplifying assumptions and often they may not yield accurate results. The stiffness properties such as elastic constants are based on integration of the properties and geometric information over the volume of the unit cell of the foam. In that case, analytical methods can yield reasonable estimates of the elastic constants of the foam. On the other hand, strength and fracture toughness are based on local failure of foam ligaments. In such situations, analytical models are found to be inadequate.

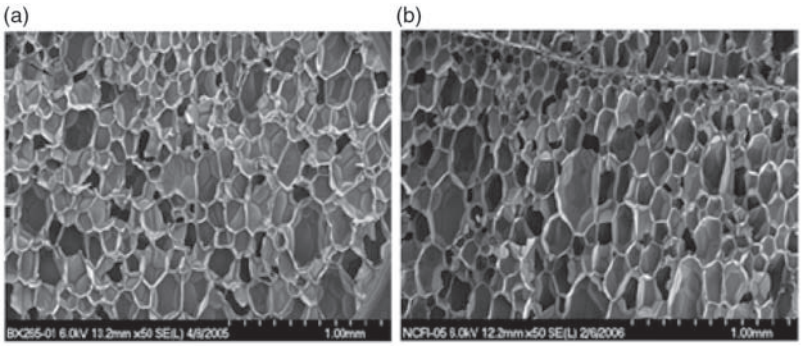

Figure 1. Photomicrographs of foams used in insulation of external fuel tanks of space vehicles. (a) BX-265 and (b) NCFI24-124.[1]

In this paper, we develop an FE-based micromechanical analysis for estimating the elastic constants and failure stresses of foams with tetrakaidecahedral unit cells. The results from the FE analysis which can model the foam ligaments accurately are compared with models including analytical models that approximate the cross section of the ligaments. The results indicate the importance of accurately modeling the foam microstructure for predicting the stiffness and strength of the foam, especially the strength properties.

FE modeling of a tetrakaidecahedron cell

The tetrakaidecahedron is a polyhedron with 14 faces, 24 vertices, and 36 edges. It is obtained by truncating the corners of an octahedron, and hence also referred to as a truncated octahedron. The equisided tetrakaidecahedral cell, obtained by truncating a cube, is a 14-faced figure made up of 8 hexagonal faces and 6 square faces. The 36 struts or ligaments, in an equisided tetrakaidecahedron, are equal in length. The cross section of the strut, which is an equilateral triangle, varies along the length.

An FE model of the tetrakaidecahedral unit cell has been described by Thiyagasundaram et al.[6,7] is shown in Figure 2. The principal directions, X, Y, and Z are assumed to be along the centers of the six squares. The six squares correspond to the front and back, the left and right, and the top and bottom, respectively. They used both Euler-Bernoulli beam and shear deformable beam elements to model the struts. Two different types of cross sections can be considered: equilateral triangle and three-cusped equilateral triangle. It was found that the classical beam element overpredicts the stiffness of the foam and shear deformable beam element is required, especially if the slenderness ratio of the foam ligaments is less than 10.

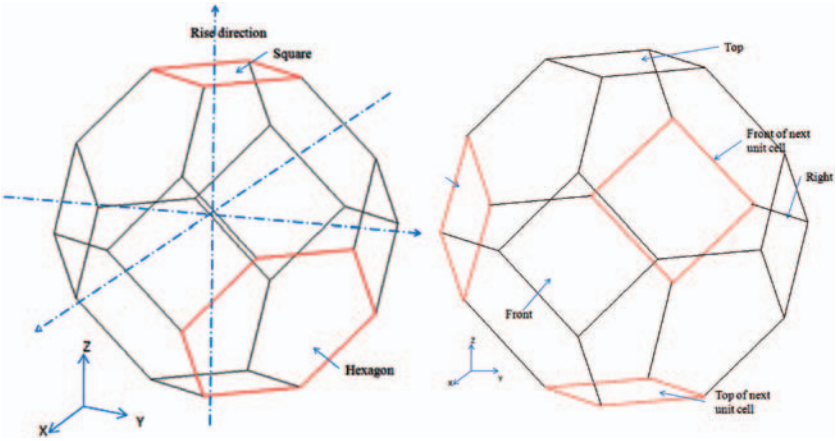

Figure 2. Equisided tetrakaidecahedron—beam model with 24 struts.

Periodic boundary conditions were imposed on the nodes of the unit cell to achieve a given state of macrostrain. The periodic boundary conditions are applied to the three translational and three rotational degrees of freedom of the opposite pairs of nodes on the squares of the unit cell as shown in Figure 3. For an applied deformation gradient $\varepsilon_{ij} = u_{i,j} = \bar{\varepsilon}_{ij}$, the nonzero periodic boundary conditions are given by

$$\bar{\varepsilon}_{ij} = \frac{1}{V}\left(u_i^{(+j)} - u_i^{(-j)}\right)A_j \tag{1}$$

where $u_i^{(+j)}$ and $u_i^{(-j)}$ are the u_i displacement on the pair of opposite faces normal to the j-direction, A_j is the area of the face normal to the j-direction in the unit cell,

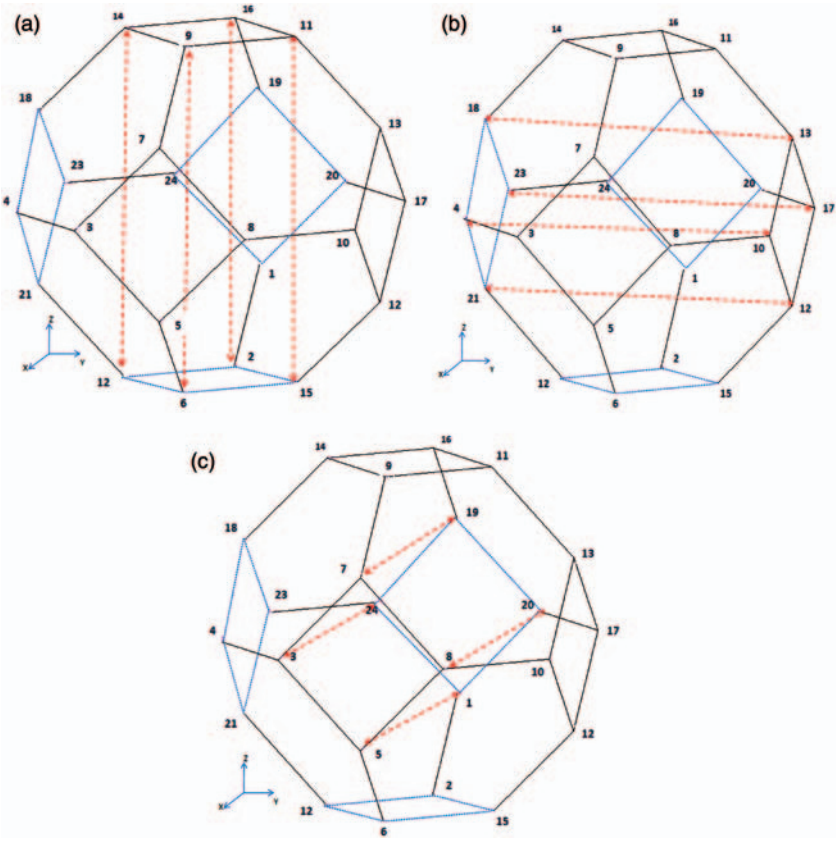

Figure 3. Nodal pairs subjected to periodic boundary conditions. The dashed lines indicate corresponding pairs. (a) Top and Bottom (b) Right and left and (c) front and back.

and V is the volume of the unit cell. For example, the periodic boundary condition corresponding to the normal strains is given by

$$\bar{\varepsilon}_{ii} = \frac{\left(u_i^{(+i)} - u_i^{(-i)}\right)}{a_i} (i = 1, 2, 3; \text{ no summation over } i) \tag{2}$$

where a_i is the dimension of the unit cell in the ith direction. The periodic boundary conditions corresponding to the rotational degrees of freedom take the form

$$\left(\theta_i^{(+j)} - \theta_i^{(-j)}\right) = 0 \ (i, j = 1, 3) \tag{3}$$

Derivation of the elastic constants

The representative volume element (RVE) shown in Figure 4 of the foam is a cuboid and because of symmetry about the three planes, the foam will behave as an orthotropic material in macroscale. In the equivalent orthotropic material, the principal material directions are parallel to the edges of the cuboid and the normal and shear deformations are uncoupled. The macroscale stress–strain relations of the foam are written as

$$\begin{Bmatrix} \sigma_1 \\ \sigma_2 \\ \sigma_3 \end{Bmatrix} = \begin{bmatrix} C_{11} & C_{12} & C_{13} \\ C_{21} & C_{22} & C_{23} \\ C_{31} & C_{32} & C_{33} \end{bmatrix} \begin{Bmatrix} \varepsilon_1 \\ \varepsilon_2 \\ \varepsilon_3 \end{Bmatrix}$$
$$\tau_{23} = G_{23}\gamma_{23}, \ \tau_{31} = G_{31}\gamma_{23}, \ \tau_{23} = G_{23}\gamma_{23} \tag{4}$$

The details of the micromechanics approach for determining the elastic constants C_{ij} can be found in Reference [6]. Here, we summarize the key steps for the sake of completion and also for subsequent discussion. When the RVE is subjected to three independent deformations such that in each case only one normal strain is nonzero and other two normal strains are zero (e.g. $\varepsilon_1 = 1$, $\varepsilon_2 = 0$, and $\varepsilon_3 = 0$), the corresponding force resultants in the three faces of the unit cell normal to the 1, 2, and 3 directions are, respectively, F_{11}, F_{21}, and F_{31}. Then, the corresponding macrostresses are obtained as

$$\sigma_1 = \frac{F_{11}}{A_1}, \ \sigma_2 = \frac{F_{21}}{A_2}, \ \sigma_3 = \frac{F_{31}}{A_3} \tag{5}$$

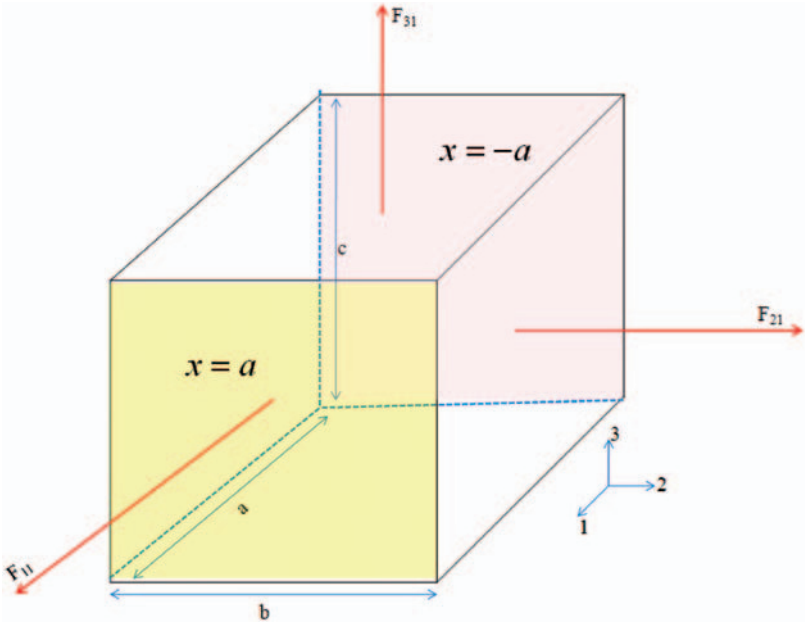

Figure 4. Representative volume element (RVE) showing force resultants in the three directions when subjected to normal strain in the 1-direction on the two faces given by $x = a$ and $x = -a$.

where A_1, A_2, and A_3 are areas normal to the 1, 2, and 3 directions. Substituting for the macrostresses and strains in equation (4) we obtain

$$C_{11} = F_{11},\ C_{21} = F_{21},\ C_{31} = F_{31} \tag{6}$$

The second and third columns of the [C] matrix are filled following similar procedures.[6] In order to determine the shear modulus, we again apply the corresponding periodic boundary conditions. The shear modulus G_{ij} is determined by equating the strain energy in the unit cell obtained from the FE analysis to the shear strain energy in terms of macroscale shear strains

$$U = \frac{1}{2} G_{ij} \gamma_{ij}^2 V \quad \text{or} \quad G_{ij} = \frac{2U}{\gamma_{ij}^2 V} \tag{7}$$

Determination of strength properties

The micromechanics procedures described above can be used to determine the multiaxial strength properties of the foam. The method called the direct

micromechanics method (DMM) has been used to determine the failure envelopes of composite materials[8] and cellular materials.[9] Consider a state of macrostress given by $\{\sigma_a\} = \{\sigma_x\ \sigma_y\ \sigma_z\ \tau_{yz}\ \tau_{zx}\ \tau_{xy}\}^T$. The macrostrains due to the above stress state can be calculated as $\{\varepsilon\} = [C]^{-1}\{\sigma\}$. The above macrostrain $\{\varepsilon\}$ can be represented as $\{\varepsilon\} = \{\varepsilon_x\ \varepsilon_y\ \varepsilon_z\ \gamma_{yz}\ \gamma_{zx}\ \gamma_{xy}\}^T$. We use the periodic boundary conditions in equation (2) to create the above state of macrostrains in the unit cell. Then, the FE-based micromechanics is used to determine the microstresses at various points at several cross sections of the 24 struts in the unit cell. Assuming we have a failure criterion for the strut material, we can calculate a load factor for each point defined as

$$\lambda_i = \frac{\sigma_e^f}{\sigma_e^i} \tag{8}$$

where λ_i is defined is the load factor for the ith point, σ_e^f is the strength of the strut material in terms of an effective stress, and σ_e^f is the corresponding effective stress at the ith point. In fact λ_i can be thought of as a factor of safety for the given applied macrostress state $\{\sigma_a\}$. For example, the effective stress is the von Mises stress for ductile materials; whereas, the maximum principal stress will be the effective stress for brittle materials. One can calculate the actual load $\lambda^*\{\sigma_a\}$ that will cause the first failure in any of the struts. The load factor λ^* is obviously the minimum of all λ's, that is

$$\lambda^* = \min(\lambda_1,\ \lambda_2,\ \cdots) \tag{9}$$

Then the state of stress that will cause failure of the foam is given by

$$\left\{\sigma_a^*\right\} = \lambda^*\{\sigma_a\} \tag{10}$$

A failure envelope can be created by considering several stress states $\{\sigma_a\}$. For example, the uniaxial strength in the 1-direction could be determined by using $\{\sigma_a\} = \{1\ 0\ 0\ 0\ 0\ 0\}^T$. A biaxial failure envelope in the $(\sigma_1 - \sigma_2)$ plane can be obtained using

$$\{\sigma_a\} = \left\{\cos\phi \quad \sin\phi \quad 0 \quad 0 \quad 0 \quad 0\right\}^T \tag{11}$$

where the phase angle ϕ defines the stress ratio $\sigma_2/\sigma_1 = \tan\phi$. By varying ϕ from 0 to 2π, one can construct the failure envelope in the $(\sigma_1 - \sigma_2)$ plane.

One should note that the aforementioned approach for determining the strength will not be valid for compressive strength. Cellular materials fail due to buckling of the struts under compressive loading. Analysis of a single unit cell is not sufficient to understand the compressive behavior of foams. Chung and Waas[10] studied the compressive response of cellular media using both experimental and

computational simulation. Their FE models captured the progressive localization of deformation and ensuing variation of stiffness of the foam.

Analytical models

An analytical model for foams with equisided tetrahedrons as unit cell was developed by Zhu et al.[11] The method was modified for foams with elongated tetrakaidecahedral unit cells by Sullivan et al.[1] Li et al.[12] used energy methods to calculate the Young's modulus and Poisson ratios of open cell foams with tetrakaidecahedral unit cells. They used their model to perform a parametric study. Sihn and Roy[13] used FE analysis to model the unit cell of open cell carbon foam in great detail including the anisotropic properties. They varied the microstructural properties to understand their effects on the macroscopic properties. The expressions for the Young's modulus and shear modulus for equisided tetrakaidecahedral foams derived by Zhu et al. are as follows:

Young's modulus, E_{100}

$$\frac{1}{E_{100}} = \frac{1}{6\sqrt{2}}\left(\frac{12L^2}{EA} + \frac{L^4}{EI}\right) \tag{12}$$

Poisson ratio, ν_{12}

$$\nu_{12} = 0.5\left(\frac{AL^2 - 12I}{AL^2 + 12I}\right) \tag{13}$$

Shear modulus, G_{12}

$$\frac{1}{G_{12}} = \frac{2\sqrt{2}L^2}{EA} + \frac{2\sqrt{2}L^4}{6EI}\left(\frac{8EI + GJ}{5EI + GJ}\right) \tag{14}$$

The above formulae assume the cross-sectional properties of the strut, namely, the axial rigidity, EA; bending rigidity, EI; and torsional rigidity, GJ, to be uniform in the struts. However, as discussed in the next section, the cross-sectional properties change drastically over the length of the strut. Hence, we need to perform further evaluation to determine: (a) the effects of the above simplifying assumption on the stiffness and strength properties of the foam and (b) the equivalent section properties that will give reasonable stiffness and strength estimates for a given microstructure.

Effect of varying cross section

Experimental observations[14] have shown that the strut cross sections in a foam are not uniform but vary gradually from the center toward the ends as shown in Figure 5. An example such variation is given by Reference [14]

$$A(x) = A_0 f(x) = A_0\left(86\frac{x^4}{L^4} + \frac{x^2}{L^2} + 1\right) \tag{15}$$

where A_0 is the area of cross section at the midspan of the strut, L is the length of the strut, and x is any point along the length of the strut $\left(-\frac{L}{2} \le x \le +\frac{L}{2}\right)$. The second moment of inertia and the polar moment of inertia of the strut cross section also vary as a function of the position along the strut given by

$$\begin{aligned} I(x) &= I_0\left(86\left(\frac{x}{L}\right)^4 + \left(\frac{x}{L}\right)^2 + 1\right)^2 \\ J(x) &= J_0\left(86\left(\frac{x}{L}\right)^4 + \left(\frac{x}{L}\right)^2 + 1\right)^2 \end{aligned} \tag{16}$$

where I_0 and J_0 are the sectional properties at the midpoint of the strut $x = 0$. When the strut cross section is an equilateral triangle of side d, the cross-sectional properties are given by

$$A = \frac{\sqrt{3}}{4}d^2,\ I = \frac{\sqrt{3}}{96}d^4,\ J = \frac{A^2}{5\sqrt{3}} \tag{17}$$

The variation of A and I are plotted in nondimensional form in Figure 6(a) and (b), respectively. It should be mentioned that $J(x)/J_0 = I(x)/I_0 = f^2(x)$.

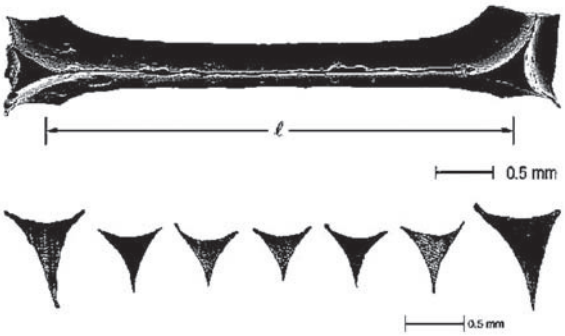

Figure 5. Varying of cross section in a strut.[14]

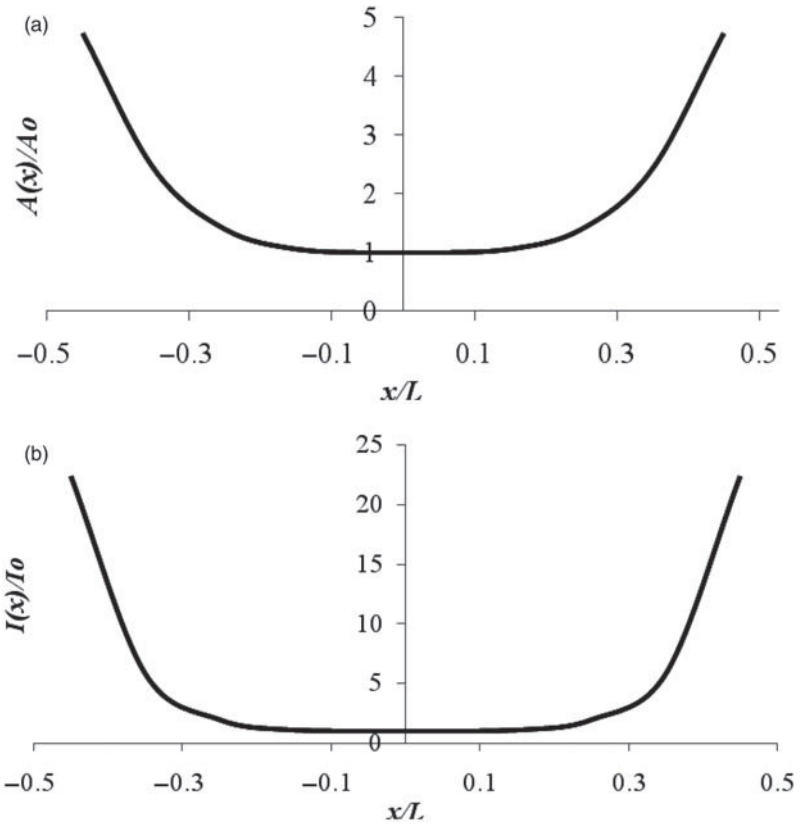

Figure 6. Variations of $A(x)/A_0$ and $I(x)/I_0$ along the length of the strut. (a) $A(x)/A_0$ vs. x/L and (b) $I(x)/I_0$ vs. x/L.

Equivalent cross-sectional properties

As discussed earlier, there are some advantages in idealizing a foam as having constant cross section for the struts. In the following, we will discuss three different methods of determining the equivalent cross-sectional properties.

Equivalent density method

In this approach, we match the relative densities of the actual foam and the idealized foam. Using the relation of the type given in equation (15), we can derive an expression for the uniform cross-sectional area as

$$A_{avg} = \frac{1}{L}\int_{-L/2}^{+L/2} A(x)dx = A_0 \int_{-1/2}^{+1/2} f(\xi)d\xi, \text{ where } \xi = \frac{x}{L} \tag{18}$$

Once the average cross-sectional area is established, the average cross-sectional dimensions can be determined. Assuming the cross section as an equilateral triangle, we can obtain the side of the triangle and I and J using equation (17). One should note that there is no mechanistic explanation for this method.

Harmonic averaging

In the second method, we match the axial, torsional, and bending rigidities of the actual strut and the idealized strut. Consider the case of axial deformation of the strut. The axial force P is constant in the strut. We will match the strain energy due to the axial force in both actual and ideal struts as

$$\frac{P^2 L}{2\bar{A}E} = \int_{-L/2}^{+L/2} \frac{P^2}{2A(x)E} dx \tag{19}$$

Then, we obtain the cross-sectional area $\bar{A}$ of the equivalent struts as

$$\frac{1}{\bar{A}} = \frac{1}{A_0} \int_{-1/2}^{1/2} \frac{1}{f(\xi)} d\xi \tag{20}$$

The above approximation is exact, as the axial force is constant in the strut in the actual foam. A similar argument could be made for torsional rigidity also as the torque remains constant both in the actual foam and idealized foam. The equivalent polar moment of inertia and bending rigidity are derived as

$$\frac{1}{\bar{J}} = \frac{1}{J_0} \int_{-1/2}^{1/2} \frac{1}{f^2(\xi)} d\xi \tag{21}$$

$$\frac{1}{\bar{I}} = \frac{1}{I_0} \int_{-1/2}^{1/2} \frac{1}{f^2(\xi)} d\xi \tag{22}$$

Equivalent bending rigidity (equivalent-I) approach

In the case of the bending deformation of the strut, the harmonic averaging method described above may not be accurate, because the bending moment along the length of the strut need not be constant. The formulae in equations (12) and (14) indicate that the elastic constants of the foam are strong functions of the flexural rigidity, EI, of the strut. This is not surprising because irrespective of the stresses acting on the foam (normal or shear), the foam deforms due to the bending of the struts. The axial and torsional deformations of the struts are minimal. Hence, it is

important to model the bending behavior of the strut as accurately as possible in determining the equivalent cross section. In general, the bending moment along a strut has a linear variation given by

$$M(x) = M_0 + \Delta M \frac{2x}{L} \tag{23}$$

where M_0 is the bending moment at the center of the strut and ΔM is the difference in the values of the bending moments at the two ends of the strut. The variation of $M(x)$ is depicted in Figure 7. Equating the bending energies of the constant and the varying cross-section struts, we obtain

$$\int_{-L/2}^{+L/2} \frac{(M(x))^2}{2EI(x)} dx = \frac{1}{2EI_c} \int_{-L/2}^{+L/2} (M(x))^2 dx \tag{24}$$

Substituting for $M(x)$ from equation (23), and integrating, we obtain the equivalent moment of inertia of the cross section I_c as

$$\frac{1}{I_c} = \left(1 + \frac{1}{3}\left(\frac{\Delta M}{M_o}\right)^2\right)^{-1} \left(\frac{1}{\bar{I}} + 4\left(\frac{\Delta M}{M_o}\right)^2 \frac{1}{I^*}\right) \tag{25}$$

where

$$\frac{1}{\bar{I}} = \int_{-1/2}^{+1/2} \frac{d\xi}{I(\xi)} \text{ and } \frac{1}{I^*} = \int_{-1/2}^{+1/2} \frac{\xi^2}{I(\xi)} d\xi \tag{26}$$

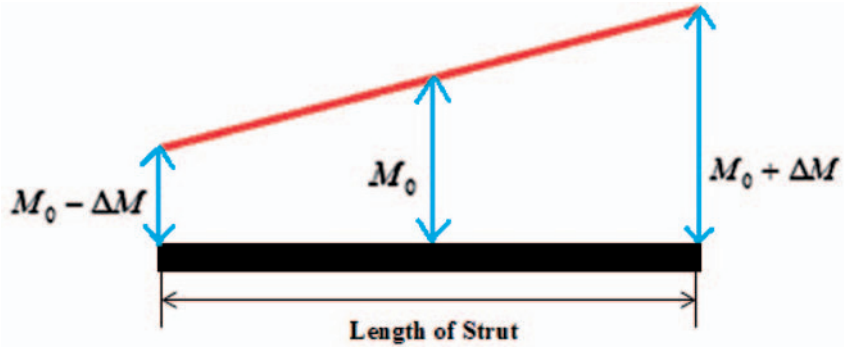

Figure 7. Depiction of linear variation of bending moment along the length of a strut.

It is to be noted that if the bending moment remains constant along the strut, that is $\Delta M = 0$, then we obtain $I_c = \bar{I}$, which is the harmonic averaging similar to that for area of cross section A and polar moment of inertia J. When $(\Delta M/M_0) \to \infty$ (which happens when $M_0 = 0$), we obtain $I_c = I^*/12$. A graph of variation of I_c with $(\Delta M/M_0)$ is shown in Figure 8. In this example, we have used $I_0 = 5.06208 \times 10^{-20}\,\mathrm{m}^4$ in the equation $I(x) = I_0(86(\frac{x}{L})^4 + (\frac{x}{L})^2 + 1)^2$. For this case, $\bar{I} = 9.78 \times 10^{-20}\mathrm{m}^4$ and $I^* = 3.01 \times 10^{-18}\mathrm{m}^4$. Thus, we note that the equivalent moment of inertia of the constant cross-section strut could vary from $9.78 \times 10^{-20}\,\mathrm{m}^4$ to $25 \times 10^{-20}\,\mathrm{m}^4$.

Results and discussion

The methods described above were used to determine the elastic constants and strength properties and also biaxial failure envelopes of foams with tetrakaidecahedral unit cell. The properties of the struts are given in Tables 1 and 2. The cross section is assumed to be equilateral triangle and the variation of cross-sectional properties is according to equations (15) and (16). The analyses of the actual foam as well as the equivalent foams were performed using the ABAQUS® FE software. The strut material was assumed to be isotropic with Young's modulus equal to 2.34 GPa and Poisson's ratio equal to 0.3. The maximum principal stress theory was used to determine the failure of the strut material, and the strength was assumed to be equal to 234 MPa. The microstresses in the struts were calculated

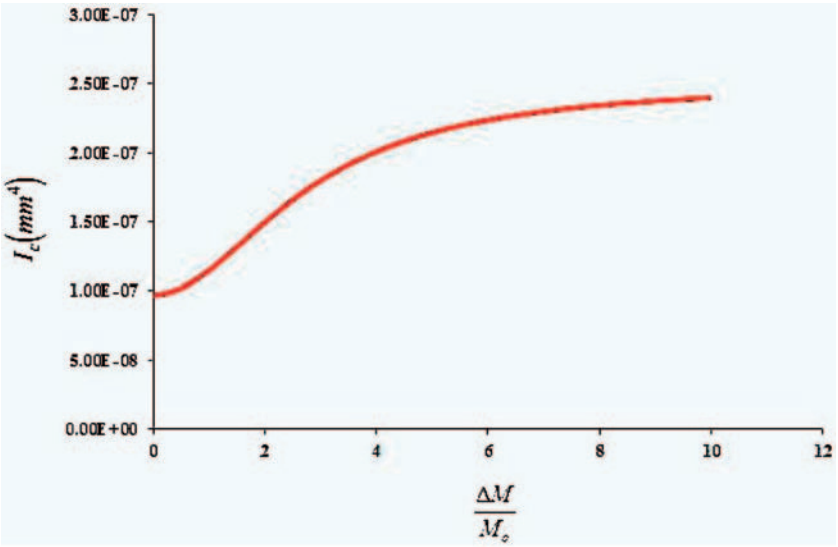

Figure 8. Variation of I_c with $\left(\frac{\Delta M}{M_o}\right)$ along the length of the strut.

Table 1. Values of side of the equilateral triangle, area of cross section, second moment of inertia, and polar moment of inertia at the midpoint of the varying cross-section strut

d_0	0.04×10^{-3} m
A_0	7.34×10^{-10} m^2
I_0	5.19×10^{-20} m^4
J_0	6.23×10^{-20} m^4

Table 2. Values of side of the equilateral triangle, area of cross section, second moment of inertia, and polar moment of inertia of the equivalent uniform cross-section strut

d_{eqv}	0.06×10^{-3} m
A_{eqv}	1.5588×10^{-9} m^2
I_{eqv}	2.3382×10^{-19} m^4
J_{eqv}	2.8059×10^{-19} m^4

at 10 cross sections in each strut and at 12 points in each cross section. Thus, the maximum principal stress was calculated at 2880 points in the unit cell of the foam.

The results are summarized in Table 3. The exact solution corresponds to the foam with varying cross section. In the varying cross-section model, each strut was modeled using 10 three-node shear deformable beam elements. The cross section of each element is assumed to be uniform and the cross-sectional property at the midpoint of an element was considered as the average property for that element. In the case of ideal foams with uniform cross-section strut, we need only one beam element for each strut.

The following observations can be made for the results in Table 3. The Young's modulus predicted by the equivalent-density method matches the Young's modulus of the actual foam (varying cross-section struts). However, the other two methods of estimating the uniform cross-section properties do not yield good results. When it comes to shear modulus, none of the approximate methods predict the shear modulus correctly. In fact the errors are so large that one needs to model the struts in detail to obtain the correct shear modulus. This is an important factor from the view point of sandwich structures because in sandwich construction the shear modulus of the foam plays a significant role in the transverse shear stiffness of the panel. All methods predict a Poisson's ratio close to 0.5, which indicates that the foam is almost incompressible. Again, all approximate models with uniform cross-section struts overpredict the tensile strength of the foam. It is not surprising because, unlike stiffness, the strength

Table 3. Comparison of results for stiffness and strength obtained using different equivalent cross-section foams

		Uniform cross section			
				Equivalent *I* method	
Property	Varying cross section (exact solution)	Equivalent density method	Harmonic averaging method	$\frac{\Delta M}{M_0} = 0$ $(I = \bar{I})$	$\frac{\Delta M}{M_0} \to \infty$ $(I = I^*)$
Young's modulus (Pa)	46.645	46.402	19.172	19.328	49.813
Shear modulus (Pa)	9888	14.920	6183	6457	16.500
Poisson's ratio	0.4986	0.4975	0.4989	0.4988	0.4981
Tensile strength (Pa)	885	2190	NA	2328	2160
Shear strength (Pa)	758	2000	NA	763	647

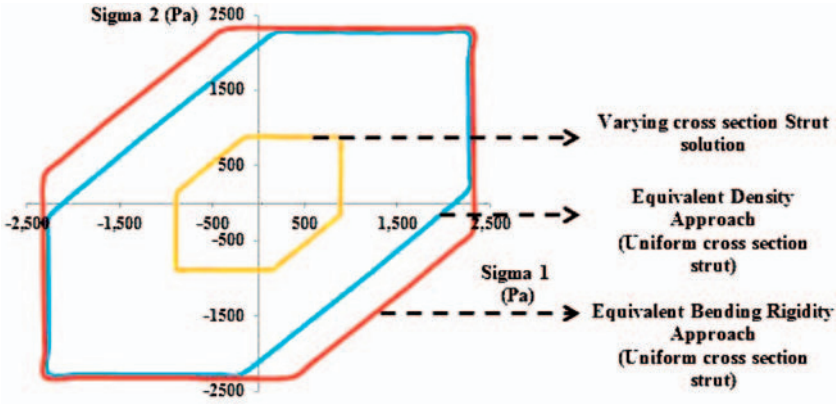

Figure 9. Comparison of biaxial failure envelopes for different models.

is determined by the weakest link in the chain or, in the present case, the weakest cross section. The uniform cross-section struts have areas that are significantly above the smallest area of the varying cross-section strut. For example, in the actual foam, the minimum dimension of the equilateral triangle is given by $d_{\min} = 0.4\,\text{mm}$. The side of the triangle in the equivalent density foam is $d_{\text{average}} = 0.6\,\text{mm}$. Thus, the moment of inertia of the cross section is about five times that of the corresponding minimum. Furthermore, the stresses for a given bending moment vary as inverse of d^3. Hence, the stresses in the actual foam could be

3.4 times that in the equivalent foam. In fact the actual tensile strength of the foam is about 2.5 times less than that predicted by approximate methods. The equivalent density model overpredicts the shear strength. The equivalent-I models do a reasonable job in predicting the shear strength, although it should be considered fortuitous coincidence considering they do not predict the elastic constants or the tensile strength accurately. The biaxial failure envelopes obtained using various methods are shown in Figure 9. Based on the discussion from tensile strength, it is not surprising none of the approximate methods could be closer to the actual failure envelope.

One may note that strength values are not given for the harmonic averaging method (see Table 3). The reason is as follows. This method directly gives the equivalent section properties such as A, I, and J which are required for the FE analysis. There is no unique cross-sectional dimension d (side of the equilateral triangle) for the given set of cross-sectional properties, and hence one cannot determine the microstresses in the struts, which govern the failure of the foam.

Conclusions

Analytical models for estimating the elastic constants of foams with tetrakaidecahedral unit cells tend to assume that the struts are of uniform cross section to facilitate easy calculation. An FE analysis taking into account the varying cross section of the strut was performed to predict the stiffness and strength properties. Three different approaches were used to determine the equivalent cross-sectional properties in the uniform strut model. The results indicate that it is possible to estimate the Young's moduli and Poisson ratios of the foam using analytical models. Accurate prediction of the shear modulus and strength properties requires detailed modeling of the strut. FE-based micromechanics will also have the advantage of modeling the anisotropic and nonlinear behavior of the strut material.

Funding

This project was supported by the National Aeronautics and Space Administration through the University of Central Florida's NASA-Florida Space Grant Consortium.

Acknowledgments

The authors acknowledge the support and encouragement of Dr. Jaydeep Mukherjee, Director and Sreela Mallick, Associate Director, FSGC.

References

1. Sullivan RM, Ghosn LJ and Lerch BA. *An elongated tetrakaidecahedron model for open celled foams*. NASA Technical Memorandum 214931, National Aeronautics and Space Administration, Glenn Research Center, Cleveland, Ohio 44135, USA, 2007.
2. Blosser ML. *Advanced metallic thermal protection systems for reusable launch vehicles*. Doctoral Dissertation, Department of mechanical and Aerospace Engineering, University of Virginia, Charlottesville, VA, USA, 2000.

3. Zhu H and Sankar BV. Analysis of sandwich TPS panel with functionally graded foam core by Galerkin method. *Compos Struct* 2007; 77: 280–287.
4. Martinez OA, Sankar BV, Haftka RT, et al. Micromechanical analysis of composite corrugated-core sandwich panels for integral thermal protection systems. *AIAA J* 2007; 49: 2323–2336.
5. Ricciardo M. *Comparison of a lattice structure cylindrical heat exchanger relative to an equivalent tubular heat exchanger*. Master's Thesis, University of Florida, Gainesville, FL, USA, 2005.
6. Thiyagasundaram P, Sankar BV and Arakere NK. Elastic properties of open-cell foams with tetrakaidecahedral cells using finite element analysis. *AIAA J* 2010; 48(4): 818–828.
7. Thiyagasundaram P, Wang J, Sankar BV, et al. Fracture toughness of foams with tetrakaidecahedral unit cells using finite element based micromechanics. *Eng Fract Mech* 2011; 78: 1277–1288.
8. Karkkainen RL and Sankar BV. A direct micromechanics method for failure analysis of plain weave textile composite. *Compos Sci Technol* 2006; 66: 137–150.
9. Thiyagasundaram P. *Material characterization of open-cell foams by finite element based micromechanics methods*. Doctoral Dissertation, University of Florida, Gainesville, FL, USA, 2010.
10. Chung J and Waas AM. In-plane biaxial crush response of polycarbonate honeycombs. *J Eng Mech* 2001; 127: 180–193.
11. Zhu HX, Knott JF and Mills NJ. Analysis of the elastic properties of open cell foams with tetrakaidecahedral cells. *J Mech Phys Solids* 1997; 45(3): 319–343.
12. Li K, Gao XL and Roy AK. Micromechanics model for three-dimensional open-cell foams using a tetrakaidecahedral unit cell and Castigliano's second theorem. *Compos Sci Technol* 2003; 63: 1769–1781.
13. Sihn S and Roy AK. Modeling and prediction of bulk properties of open-cell carbon foam. *J Mech Phys Solids* 2004; 52: 167–191.
14. Gong L, Kyriakides S and Jang WY. Compressive response of open-cell foams. Part I: morphology and elastic properties. *Int J Solids Struct* 2005; 42: 1355–1379.